Competing Pathways in the 248 nm Photodissociation of Propionyl Chloride and the Barrier to Dissociation of the Propionyl Radical†

Laura R. McCunn, Maria J. Krisch, Kana Takematsu, and Laurie J. Butler*

The James Franck Institute and Department of Chemistry, The University of Chicago, Chicago, Illinois 60637

Jinian Shu

Chemical Sciences Division, Lawrence Berkeley National Laboratory, Berkeley, California 94720

Received: January 25, 2004; In Final Form: April 13, 2004

Photofragment translational spectroscopy was used to study the photodissociation of propionyl chloride at 248 nm. The crossed laser-molecular beam experiment with VUV photoionization showed two primary dissociation channels, C−Cl bond fission and HCl elimination. Following cleavage of the C−Cl bond, unimolecular dissociation of the propionyl radical produced CH_3CH_2 and CO. The energy barrier to the $CH_3CH_2CO \rightarrow CH_3CH_2 + CO$ reaction was estimated to be in the range of 16.3 ± 1.5 kcal/mol by determining the internal energy distribution of surviving propionyl radicals. No other secondary dissociation channels were observed for the propionyl radical. The HCl elimination channel, previously reported only for the condensed phase of propionyl chloride, was observed as the minor primary dissociation channel in the gas phase. The cofragment to the HCl elimination, CH_3CHCO or CH_2CH_2CO, underwent secondary dissociation to produce CO and CH_2CH_2 with a significant amount of energy partitioned into translational motion.

Introduction

This paper reports the photofragment translational spectroscopy of propionyl chloride, $CH_3CH_2C(O)Cl$, photodissociated at 248.5 nm. The experiments resolve the competing product channels in the primary dissociation of propionyl chloride and determine the energy barrier for secondary dissociation of the propionyl radical. Previous studies of the photolysis of gas-phase propionyl chloride[1] and analogous propionyl compounds[2,3] have focused on the formation of the propionyl radical. Meanwhile, the existence of an elimination channel, producing CH_3CHCO or CH_2CH_2CO, has not been adequately investigated. The propionyl radical, which can be generated by photocleavage of the C−Cl bond, has received considerable attention because of the significance of acyl radicals to combustion processes and atmospheric chemistry.[1,4,5] In addition, there is interest in the $CH_3CH_2CO \rightarrow CH_3CH_2 + CO$ reaction because of its non-statistical behavior.[2,3,6,7]

There are several energetically allowed reactions for propionyl chloride excited at 248 nm. The most obvious primary channel, C−Cl bond fission, and the subsequent secondary reaction producing $CH_3CH_2 + CO$ have been well-documented;[1−3,5−11] however, there is a scarcity of literature examining any competing dissociation channels, either primary or secondary. The goal of the experiments described below is to determine which primary photodissociation processes occur and what secondary dissociation processes ensue in the resultant radical or molecular primary products. Listed below are the reactions that are energetically possible at 248 nm, with secondary processes indented:

$$CH_3CH_2COCl \rightarrow CH_3CH_2CO + Cl \qquad \Delta H_{0K} = 83.1 \text{ kcal/mol}^{12} \quad (1)$$

$$CH_3CH_2CO \rightarrow CH_3CH_2 + CO \qquad \Delta H_{0K} = 9.6 \text{ kcal/mol}^{12} \quad (2)$$

$$CH_3CH_2COCl \rightarrow CH_3CH_2 + COCl \qquad \Delta H_{0K} = 85.7 \text{ kcal/mol}^{12} \quad (3)$$

$$CH_3CH_2COCl \rightarrow CH_3CHCO + HCl \qquad \Delta H_{0K} = 17.5 \text{ kcal/mol}^{12} \quad (4)$$

$$CH_3CHCO \rightarrow CH_2CH_2 + CO \qquad \Delta H_{0K} = 7.7 \text{ kcal/mol}^{12} \quad (5)$$

$$CH_3CH_2COCl \rightarrow CH_2CH_2CO + HCl \qquad \Delta H_{0K} = 43.1 \text{ kcal/mol}^{12,13} \quad (6)$$

$$CH_2CH_2CO \rightarrow CH_2CH_2 + CO \qquad \Delta H_{0K} = -17.9 \text{ kcal/mol}^{13} \quad (7)$$

Studies by our group on acetyl chloride and bromoacetyl chloride explain the mechanism for α-bond cleavage of acyl chlorides.[14] Absorption of a 248 nm photon excites a $^1(\pi^* \leftarrow n)$ transition, followed by rapid crossing to a $(\sigma^* \leftarrow np)$ surface and breaking of the C−Cl bond.[12] Whereas all previously published experiments on this molecule in the gas phase have examined only the C−Cl bond fission channel, Winter et al. identified an HCl elimination channel for propionyl chloride isolated in an argon matrix at 10 K.[12] Using a polarized laser for photodissociation, they were able to show that elimination must occur by a direct mechanism, instead of H abstraction by the Cl atom.

† Part of the special issue "Richard Bersohn Memorial Issue".

* Corresponding author. E-mail: ljb4@midway.uchicago.edu.

10.1021/jp0496506 CCC: $27.50
Published on Web 00/00/0000 PAGE EST: 5.3

Studies with deuterium-labeled propionyl chloride established that the reaction proceeds strictly by α-elimination (four-centered).

Although there are a few published experiments regarding the kinetics and energy barrier of the radical dissociation $CH_3CH_2CO \rightarrow CH_3CH_2 + CO$, they date back approximately 30 years. In the earliest study, Kerr and Lloyd produced the propionyl radical by means of photolysis of azoethane in the presence of propionaldehyde. From their measurements of rate constants, they concluded that the barrier to propionyl decomposition is 14.6 kcal/mol.[9,10] Watkins and Thompson performed similar experiments with azoethane and CO and found a barrier of 14.7 kcal/mol.[8] More recently, two experimental studies[2,3] evaluated nonstatistical behavior in the dynamics of the propionyl radical dissociation and involved calculations that used a different value, 17 kcal/mol, for the dissociation barrier. This number was used based on a dissociation energy of 13 kcal/mol and the 4.8 kcal/mol activation energy[8] for the reverse addition reaction and is similar to the experimentally determined value for the $CH_3CO \rightarrow CH_3 + CO$ barrier.[15]

In response to the interest in the dynamics of propionyl radical decomposition, there have been theoretical predictions of the energy barrier to dissociation. These calculations agree most closely with the early experimental values of Kerr and Lloyd and of Watkins and Thompson. Calculations by Martinez-Nunez and Vazquez-Rodriguez predict a zero-point-corrected barrier of 14.9 kcal/mol at CBS-QB3 level.[6] Méreau et al. calculated a 15.6 kcal/mol barrier at 298 K by an ab initio G2(MP2) method and 15.8 kcal/mol by a DFT (B3LYP) method.[5]

Our experiments provide a method to determine this barrier directly by photodissociating propionyl chloride at 248.5 nm. Given the photon energy of 114.9 kcal/mol and a C−Cl bond energy of approximately 83.1 kcal/mol,[12] a portion of the nascent propionyl radicals may not have sufficient internal energy to overcome the dissociation barrier. In this paper, we report the detection of both stable propionyl radicals and the secondary dissociation products $CH_3CH_2 + CO$ of the unstable radicals and make a rough determination of the barrier to dissociation.

Experimental Method

Photofragment translational spectroscopy was performed on the rotating-source crossed laser-molecular beam apparatus on the Chemical Dynamics Beamline at Lawrence Berkeley National Laboratory's Advanced Light Source (ALS). Details of the experimental apparatus have been described previously.[16] A 6.6% propionyl chloride−He molecular beam was created by bubbling He (605 Torr total backing pressure) through propionyl chloride cooled to 12 °C and expanding it through a piezoelectric pulsed valve (0.5 mm orifice) operating at 100 Hz. The nozzle was heated to 153 °C to reduce cluster formation. The molecular beam of the parent molecule was characterized by directing the beam through a chopper wheel straight into the detector. The measured number-density velocity of the propionyl chloride molecular beam for the data presented here typically peaked at 1.3×10^5 cm/s with a fwhm of 20%.

Photodissociation was accomplished with a Lambda Physik COMPex 110 excimer laser operating at the 248.5 nm KrF transition with a pulse energy of 200 mJ/pulse. The laser beam was focused to an area of 1.8 mm × 5.0 mm, intersecting the molecular beam at a 90° angle in the interaction region. Photofragments recoiling in the direction of the detector traveled 15.1 cm to the ionizing region, where tunable VUV synchrotron radiation ionized a portion of the fragments. Photoionization energies were selected by tuning the gap of a U10 undulator, which generated the radiation. The necessary undulator gap (mm) was calculated from the desired photoionization energy, x (eV), using the following polynomial:[17]

$$\text{gap(mm)} = 7.875\text{(mm)} + 2.5054\text{(mm/eV)}x - 0.068\,545\text{(mm/eV}^2)x^2 + 0.000\,824\,77\text{(mm/eV}^3)x^3 \quad (8)$$

For example, CH_3CH_2 data at $m/e = 29$ were collected using an 11.0 eV photoionization energy, requiring a 28.238 mm undulator gap. Unwanted higher harmonics of VUV radiation were removed by an argon gas filter. The VUV beam was defined by a 10 mm × 10 mm aperture.

Ionized photofragments were mass-selected by an Extrel 2.1 MHz quadrupole mass spectrometer and then counted by a Daly detector. The total time-of-flight (TOF) from the interaction region to the detector was recorded for the photofragments. An ion flight constant of 5.72 $\mu s \cdot amu^{-1/2}$ was used to account for the time spent as ions in the detector. Recoil translational energy distributions were found by forward convolution fitting of the TOF spectra.

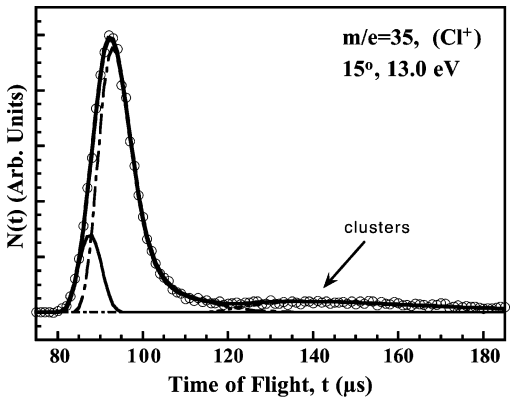

Figure 1. TOF spectrum for $m/e = 35$ (Cl^+) from the photodissociation of propionyl chloride at 248 nm. Open circles represent experimental data taken at 13.0 eV photoionization energy and a source angle of 15° for 20 000 laser shots. The thin solid line fits high recoil kinetic energy chlorine atoms with momentum-matched propionyl radicals that are stable to secondary dissociation. The low recoil kinetic energy chlorine atoms are fit by the long-dash−dotted line. The short-dash−dotted line shows signal from clusters. The thick solid line is the overall forward convolution fit using the $P(E_T)$ in Figure 2.

Results and Analysis

The data evidenced that both C−Cl bond fission and HCl elimination occur in the photodissociation of propionyl chloride at 248 nm. C−Cl fission was evidenced by the Cl^+ signal at $m/e = 35$ shown in Figure 1.

The total recoil kinetic energy bimodal distribution $P(E_T)$ in C−Cl fission was determined by forward convolution fitting of the data and is shown in Figure 2. The high recoil kinetic energy Cl atoms momentum-match to low internal energy propionyl radicals that do not undergo secondary dissociation. The Cl atoms with low recoil kinetic energy correspond to the momentum-matched propionyl radicals with high internal energy that is sufficient for secondary dissociation. The E_T marking the onset of dissociation of the unstable propionyl radicals gave us an estimate of the energy barrier to dissociation, as described in the Discussion. A signal from cluster fragments also appeared in the $m/e = 35$ TOF. Despite increasing the nozzle temperature by 40 °C to 153 °C, the cluster signal could not be completely eradicated.

A TOF spectrum taken at $m/e = 36$ ($H^{35}Cl^+$) and a 30° source angle (Figure 3) indicated the presence of an HCl elimination

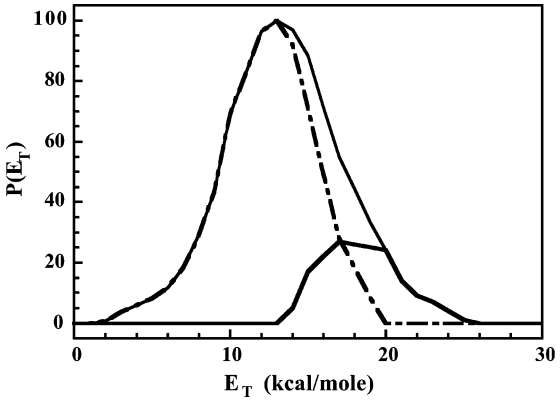

Figure 2. Unnormalized $P(E_T)$ for C−Cl bond fission at 248 nm derived from the forward convolution fitting of the $m/e = 35$ TOF spectrum shown in Figure 1. The bold solid line shows the high recoil kinetic energy C−Cl bond fission and the dash−dotted line corresponds to low recoil kinetic energy. The total $P(E_T)$ is shown by the solid line.

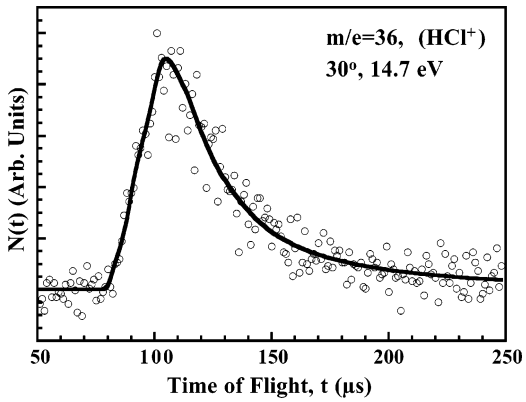

Figure 3. TOF spectrum of $m/e = 36$ (HCl^+) taken at 14.7 eV photoionization energy and a source angle of 30° for 30 000 laser shots. Open circles represent experimental data and the solid line is the forward convolution fit using the $P(E_T)$ in Figure 4.

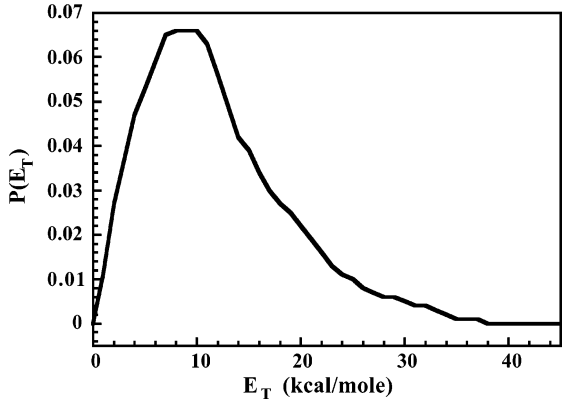

Figure 4. Normalized $P(E_T)$ for HCl elimination derived from the forward convolution fitting of the $m/e = 36$ (HCl^+) TOF spectrum shown in Figure 3.

channel. The data were fit by a single $P(E_T)$, shown in Figure 4, which was slower and broader than the C−Cl bond fission $P(E_T)$ (Figure 2). To determine a rough branching ratio between Cl^+ and HCl^+, we integrated the signal in the respective background-subtracted TOF spectra. A $m/e = 35$ (Cl^+) TOF spectrum taken at a 30° source angle with an ionization energy of 15.0 eV and 14.2 mW power was integrated in the range of 75−130 μs, excluding signal from clusters. This is not the TOF spectrum shown in Figure 1, as we chose Cl^+ and HCl^+ spectra

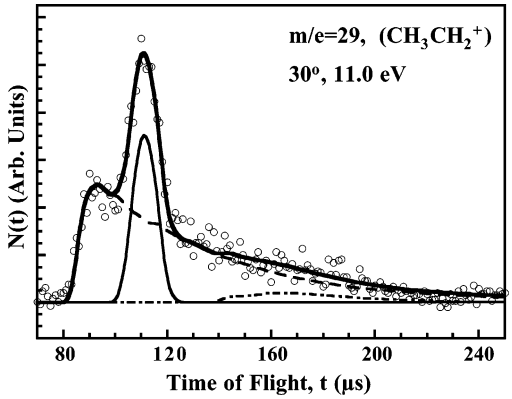

Figure 5. TOF spectrum for $m/e = 29$ ($CH_3CH_2^+$) at 248 nm. Open circles represent experimental data taken at 11.0 eV photoionization energy and a source angle of 30° for 100 000 laser shots. The bold solid line is the overall forward convolution fit using the $P(E_T)$ in Figure 6. Ethyl radicals produced from secondary dissociation of slow propionyl radicals are shown by the dashed line. The thin solid line shows fast, stable propionyl radicals that fragment to $m/e = 29$ in the ionizer. The dash−dotted line shows signal contribution from clusters.

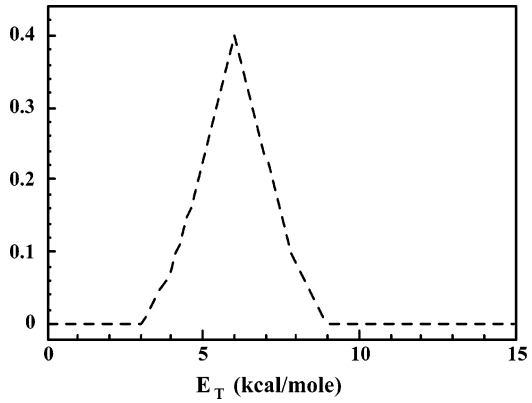

Figure 6. Normalized $P(E_T)$ for dissociation of the propionyl radical derived from the forward convolution fitting of the $m/e = 29$ ($CH_3CH_2^+$) TOF spectrum shown in Figure 5.

that were collected on the same day, with identical beam conditions and the same source angle. The $m/e = 36$ (HCl^+) TOF spectrum at a 30° source angle with 14.7 eV ionization energy (10.6 mW) was integrated from 60 to 200 μs. Accounting for the appropriate Jacobian factors and normalizing for ALS photoflux gave a [Cl]/[HCl] branching ratio of 6.5, given that the photoionization cross sections of Cl and HCl are nearly equal.[18,19] The determination is qualitative, as it could not account for the fact that other data we have taken show that the HCl^+ signal is not linear in ALS power.[20] We looked for evidence of C−C bond fission by examining the TOF spectrum for $m/e = 63$ ($COCl^+$) at a 15° source angle and 15.0 eV ionization energy. No signal above the noise was observed after 50 000 laser shots. Also, all components of the signal at $m/e = 29$ ($CH_3CH_2^+$) were adequately fit by processes other than primary C−C fission, as described below.

Following cleavage of the C−Cl bond, unimolecular dissociation of the nascent propionyl radicals with high internal energies produced CH_3CH_2 and CO. Figure 5 shows the TOF for $m/e = 29$ ($CH_3CH_2^+$) at a 30° source angle. The low, fast peak of the TOF, fit by the dashed line, is the CH_3CH_2 signal from the dissociation of the propionyl radicals. The $P(E_T)$ for the $CH_3CH_2CO \rightarrow CH_3CH_2 + CO$ products was then determined to be sharply peaked at 6 kcal/mol (Figure 6). It was determined by forward convolution fitting of the TOF, accounting for both the velocity imparted to the dissociating propionyl

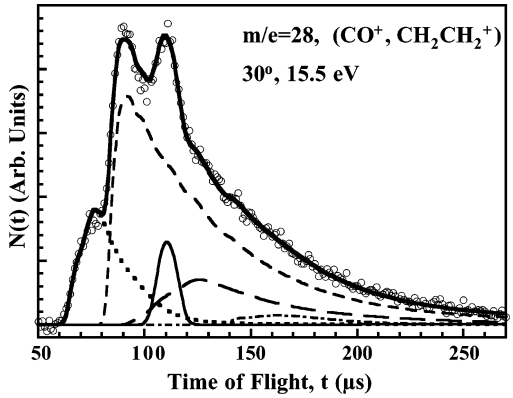

Figure 7. TOF spectrum for $m/e = 28$ (CO^+, $CH_2CH_2^+$) at 248 nm. Open circles represent experimental data taken at 15.5 eV photoionization energy and a source angle of 30° for 100 000 laser shots. The bold solid line is the overall forward convolution fit using the $P(E_T)$ in Figure 8. The dotted line is CO and CH_2CH_2 from dissociation of the C_3H_4O fragment resulting from HCl elimination. Stable C_3H_4O photofragments that crack in the ionizer to $m/e = 28$ appear at the long dashed line in the spectrum. CO produced from dissociation of slow propionyl radicals is shown by the medium dashed line. The thin solid line shows fast, stable propionyl radicals that fragment to $m/e = 28$ in the ionizer. The dash−dotted line shows signal contribution from clusters.

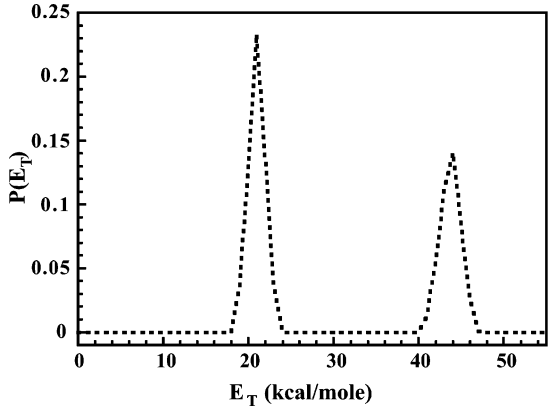

Figure 8. Normalized $P(E_T)$ for dissociation of the C_3H_4O photofragments of HCl elimination. It was determined from forward convolution fitting of the TOF spectrum in Figure 7 that a bimodal distribution best fit the data.

radicals using the dot−dashed portion of the C−Cl bond fission $P(E_T)$ in Figure 2 and the recoil of the CH_3CH_2 from the CO in the dissociation of these radicals.

The solid line component of the TOF in Figure 5 shows the signal that was fit by using the high E_T portion of the $P(E_T)$ for C−Cl fission in Figure 2. Using the full $P(E_T)$ gave an unsatisfactory fit, so it was necessary to use only the high E_T distribution from Figure 2. Although we could not find the appearance energy of $CH_3CH_2^+$ in the literature, this component is believed to come from stable propionyl radicals that fragment to $m/e = 29$ upon photoionization. There is also an appreciable contribution from clusters to TOF signal, shown by the dash−dotted line in Figure 5.

Figure 7 shows the $m/e = 28$ (CO^+, $CH_2CH_2^+$) TOF spectrum containing components derived from both the C−Cl fission and HCl elimination pathways. Most of the signal in the complicated spectrum is fit easily by kinetic energy distributions determined by the detection of other masses. The dashed line shows the signal from CO produced in the secondary dissociation of the propionyl radical (reaction 2). The $P(E_T)$, shown in Figure 6, used to fit this portion of the $m/e = 28$ signal was determined from fitting the cleaner signal from the partner fragment CH_3-CH_2. Again, propionyl radicals that are stable to secondary dissociation appear in the spectrum due to cracking in the ionizer. The fit and $P(E_T)$ for these radicals are shown by the solid line in Figures 7 and 2, respectively. The dash−dotted line shows a small signal contribution from clusters.

The only remaining undetermined signal in the spectrum is due to the C_3H_4O cofragment to the HCl elimination (reaction 4 or 6). By assuming that some of the C_3H_4O produced underwent secondary dissociation to produce CO and CH_2CH_2 (reaction 5 or 7) and some, formed in coincidence with higher translational energy HCl product, was stable to secondary dissociation, we were able to fit the remaining signal. The latter contribution was calculated from the $P(E_T)$ for HCl elimination shown in Figure 4 with the resulting fit shown by the long-dashed line in Figure 7. Although C_3H_4O formed in coincidence with high translational energy HCl should be most stable, we fit the data presuming that the fraction of stable C_3H_4O product is constant across the primary recoil kinetic energy distribution. The remaining CO and CH_2CH_2 signal from the secondary dissociation of the unstable C_3H_4O produced from HCl elimination was fit by forward convolution, giving the dotted line contribution in Figure 7. The fit accounted for the primary recoil between the HCl and C_3H_4O product using the $P(E_T)$ in Figure 4 and the recoil for the $C_3H_4O \rightarrow CH_2CH_2 + CO$ secondary process determined by forward convolution fitting of the fast signal. The $P(E_T)$ for this process is peculiar because the fast edge of the TOF could only be fit by assuming a bimodal $P(E_T)$ for the secondary dissociation, as shown by the dotted line in Figure 8. Though there was considerable latitude in the forms of the $P(E_T)$ that gave an acceptable fit of the signal, they all had a bimodal nature. This indicates that there may be two different mechanisms occurring in the secondary dissociation of the C_3H_4O fragment. The higher kinetic energy portion of the $P(E_T)$ may also be due to a multiphoton process, although we did not perform a laser power dependence study to confirm this. A substantial amount of the available energy is partitioned into the translational motion of the C_2H_4 and CO fragments. This is in accordance with the large exit barrier of 74.6 kcal/mol for the $CH_3CHCO \rightarrow CH_2CH_2 + CO$ reaction predicted by Schalley et al.[13]

Discussion

The data presented here allow for a determination of the barrier to propionyl dissociation as the Cl atom TOF determines the internal energy of all nascent propionyl radicals and the signal fit in Figure 5 indicates which of the radicals survive secondary dissociation. Then the internal energy of propionyl radical that marks the onset of secondary dissociation is found by comparing the two fits. The internal energy, E_{int}, of the propionyl radical is obtained by the following energy conservation relationship:

$$E_{parent} + E_{h\nu} = D_0(\text{C}-\text{Cl}) + E_{int} + E_{Cl} + E_T \qquad (9)$$

$E_{h\nu}$, the energy of a 248.5 nm photon, is equal to 114.9 kcal/mol, accounting for the air-to-vacuum correction. D_0(C−Cl) is taken as 83.1 kcal/mol.[12] E_{parent} is the energy of the propionyl chloride molecule; we estimate it by assuming that vibrational energy is not cooled by the nozzle expansion. Using previously published vibrational modes,[12] the average vibrational energy of a propionyl chloride molecule was calculated to be 4.0 kcal/mol at the nozzle temperature of 153 °C. E_{Cl} refers to the energy

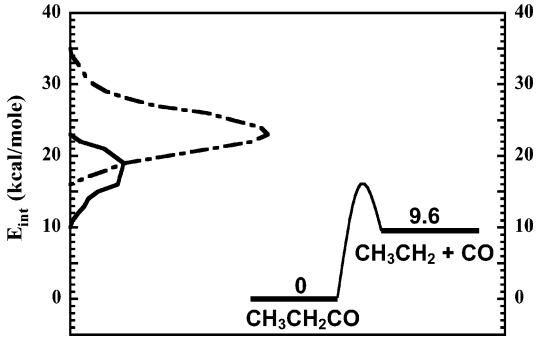

Figure 9. Internal energy (E_{int}) of the propionyl radical compared to the enthalpies of the propionyl radical and its secondary dissociation products CH_3CH_2 and CO. Enthalpies are taken from ref 12. E_{int} was calculated from $E_{h\nu} + E_{parent} = D_0(C-Cl) + E_{int} + E_{Cl} + E_T$, where E_T was taken from the $P(E_T)$ of the C−Cl bond fission channel. (Figure 2) The E_{int} shown in the figure is calculated assuming Cl ($^2P_{3/2}$), so E_{Cl} = 0 kcal/mol, but both spin−orbit states of Cl are likely produced, so we address this in the discussion. Also, E_{int} was calculated using E_{parent} = 4 kcal/mol, which does not account for the possible spread in vibrational energies of the parent molecule. The solid line corresponds to propionyl radicals that do not dissociate. These propionyl radicals correspond to Cl atoms detected at m/e = 35 (Figure 1) with high recoil kinetic energy. (Figure 2) The dash−dotted line refers to propionyl radicals with sufficient energy to overcome the secondary dissociation barrier, producing CH_3CH_2 that was detected at m/e = 29 (Figure 5) and CO detected at m/e = 28. (Figure 7) The high internal energy propionyl radicals correspond to Cl atoms produced from C−Cl bond fission with low recoil kinetic energy (Figure 2).

of the spin−orbit state of the chlorine atoms. E_{Cl} is 0 kcal/mol if Cl is produced in the $^2P_{3/2}$ state and 2.5 kcal/mol in the $^2P_{1/2}$ state.[21] Our experiments cannot distinguish between the two spin−orbit states. E_{int} is easily determined once we have measured E_T. The $P(E_T)$ for the CH_3CH_2CO + Cl recoil kinetic energy (Figure 2) shows that secondary dissociation occurs for some of the radicals from C−Cl bond fission events that partition less than 20 kcal/mol to product translation. However, it is not until about 13 kcal/mol in C−Cl recoil kinetic energy that all of the nascent propionyl radicals undergo dissociation. We attempted to fit the data with a sharp cutoff between the high and low recoil kinetic energy propionyl radicals, but did not obtain a satisfactory fit. Although one might try to explain the stability of the propionyl radicals from the lower E_T event by a centrifugal barrier to C−Cl bond fission, our calculations show that this radical is not expected to partition much energy into rotation. Using structural parameters of propionyl chloride determined at the MP2/6-311G** level of theory by Durig et al.,[22] we calculated the rotational energy to be 0.5 kcal/mol at an E_T of 13 kcal/mol. Thus, our observation that there is a range of E_T(C−Cl) over which propionyl radicals can be produced as either stable or unstable likely results from the fact that the parent internal energy is a distribution with an average of 4 kcal/mol but a significant spread. The radicals from C−Cl bond fission events that partitioned 19 kcal/mol to E_T(C−Cl) but are observed as stable in our work likely came from parent molecules with less than 4 kcal/mol vibrational energy. Figure 9 shows the internal energy distribution of the propionyl radicals and compares the value of E_{int} to the enthalpy of reaction 2. It is important to note that this figure shows E_{int} under the assumption that the propionyl radicals are formed in coincidence with Cl ($^2P_{3/2}$) and also that the parent molecules have 4 kcal/mol in vibrational energy, neglecting any possible spread in vibrational energies.

The spread in E_{parent} makes it difficult to identify the value of E_{int} that marks the barrier to dissociation. Figure 2 shows that the highest E_T for propionyl radicals that can possibly dissociate corresponds to 20 kcal/mol of C−Cl recoil kinetic energy. These radicals must also come from vibrationally hot propionyl chloride parent molecules. By eq 9 and $\langle E_{parent} \rangle$ = 4 kcal/mol, the propionyl radicals are assigned E_{int} = 15.8 kcal/mol, but these propionyl radicals likely come from parent molecules with more vibrational energy than the average, so the E_{int} is a bit higher than 16 kcal/mol. This cutoff point in the $P(E_T)$ can be seen in Figure 9. Figure 2 also shows that E_T = 13 kcal/mol marks the point where none of the nascent propionyl radicals are stable. These radicals should come from parent molecules with very little or no vibrational energy and have a Cl ($^2P_{1/2}$) cofragment in the primary photodissociation step. Experiments in our group[23] have shown that C−Cl fission that proceeds by electronic predissociation yields Cl in both spin−orbit states, so it is not unreasonable to expect Cl ($^2P_{1/2}$) produced from propionyl chloride. In this case, taking E_{parent} as 0 kcal/mol and applying eq 9 with E_{Cl} = 2.5 kcal/mol gives an E_{int} of 16.3 kcal/mol. Therefore, we assign the barrier to dissociation of propionyl radical within the range of 16.3 ± 1.5 kcal/mol.

HCl elimination could occur by α- or β-elimination, so the identity of HCl's momentum-matched partner fragment is CH_3-CHCO or CH_2CH_2CO. These two C_3H_4O fragments are indistinguishable by the technique used in this study. Winter et al. used selectively deuterated propionyl chloride in a 10 K Ar matrix to show that UV photodissociation exclusively yields HCl by α-elimination.[12] They explained this observation as likely due to a matrix effect. We plan to conduct our own experiments on deuterium-labeled propionyl chloride, CD_3CH_2-COCl, and probe for the m/e = 36 (HCl^+) or m/e = 37 (DCl^+) signal to determine if the elimination occurs by a four- or five-centered mechanism, or both. The data also show that in the internal energy range of the propionyl radical produced in this study, 10−35 kcal/mol, C−H bond fission to produce CH_3-CHCO + H does not compete to a significant extent with the C−C bond fission channel that produces CH_3CH_2 + CO. This is in agreement with the higher energy requirement for the C−H fission channel, ΔH_{0K}= 36.5 kcal/mol,[12] which is the lower limit for the reaction energy barrier and inaccessible for the range of propionyl radical internal energy.

Acknowledgment. This work was supported by the Chemical, Geosciences and Biosciences Division, Office of Basic Energy Sciences, Office of Science, U.S. Department of Energy, under Grant No. DE-FG02-92ER14305. The Advanced Light Source is supported by the Director, Office of Science, Office of Basic Energy Sciences, Materials Sciences Division, of the U.S. Department of Energy under Contract No. DE-AC03-76SF00098 at Lawrence Berkeley National Laboratory. The Chemical Dynamics Beamline is supported by the Director, Office of Science, Office of Basic Energy Sciences, Chemical Sciences Division, of the U.S. Department of Energy under the same contract. L.R.M. was partially supported by a U.S. Department of Education GAANN Fellowship. M.J.K. was supported by a NSF Graduate Research Fellowship. The authors thank David E. Szpunar for guidance during data analysis. L.J.B. acknowledges Rich Bersohn's warm collegiality and strong physical and chemical insight. He touched us all, and he lives on in the hearts of his family and his twin brother Malcolm.

References and Notes

(1) Li, H.; Li, Q.; Mao, W.; Zhu, Q.; Kong, F. *J. Chem. Phys.* **1997**, *106*, 5943.

(2) Hall, G. E.; Metzler, H. W.; Muckerman, J. T.; Presses, J. M.; Weston, R. E., Jr. *J. Chem. Phys.* **1995**, *102*, 6660.

(3) Kim, S. K.; Guo, J.; Baskin, J. S.; Zewail, A. H. *J. Phys. Chem.* **1996**, *100*, 9202.

(4) Seinfeld, J. H.; Pandis, S. N. *Atmospheric Chemistry and Physics: From Air Pollution to Climate Change*; John Wiley & Sons: New York, 1998.

(5) Mereau, R.; Rayez, M.-T.; Rayez, J.-C.; Caralp, F.; Lesclaux, R. *Phys. Chem. Chem. Phys.* **2001**, *3*, 4712.

(6) Martinez-Nunez, E.; Vazquez-Rodriguez, S. A. *J. Mol. Struct.* **2000**, *556*, 123.

(7) Martinez-Nunez, E.; Pena-Gallego, A.; Vazquez, S. A. *J. Chem. Phys.* **2001**, *114*, 3546.

(8) Watkins, K. W.; Thompson, W. W. *Int. J. Chem. Kinet.* **1973**, *5*, 791.

(9) Kerr, J. A.; Lloyd, A. C. *Chem. Commun.* **1967**, 164.

(10) Kerr, J. A.; Lloyd, A. C. *Trans. Faraday Soc.* **1967**, *63*, 2480.

(11) Chatgilialoglu, C.; Crich, D.; Komatsu, M.; Ryu, I. *Chem. Rev.* **1999**, *99*, 1991.

(12) Winter, P. R.; Rowland, B.; Hess, W. P.; Radziszewski, J. F.; Nimlos, M. R.; Ellison, G. B. *J. Phys. Chem. A* **1998**, *102*, 3238.

(13) Schalley, C. A.; Blanksby, S.; Harvey, J. N.; Schroder, D.; Zummack, W.; Bowie, J. H.; Schwarz, H. *Eur. J. Org. Chem.* **1998**, 987.

(14) Person, M. D.; Kash, P. W.; Butler, L. J. *J. Chem. Phys.* **1992**, *97*, 355.

(15) North, S. W.; Blank, D. A.; Gezelter, J. D.; Longfellow, C. A.; Lee, Y. T. *J. Chem. Phys.* **1995**, *102*, 4447.

(16) Yang, X. M.; Lin, J.; Lee, Y. T.; Blank, D. A.; Suits, A. G.; Wodtke, A. M. *Rev. Sci. Instrum.* **1997**, *68*, 3317.

(17) Peterka, D.; Ahmed, M. Personal Communication.

(18) Samson, J. A. R.; Shefer, Y.; Angel, G. C. *Phys. Rev. Lett.* **1986**, *56*, 2020.

(19) Gallagher, J. W.; Brion, C. E.; Samson, J. A. R.; Langhoff, P. W. *J. Phys. Chem. Ref. Data* **1988**, *17*, 9.

(20) Mueller, J. A.; Butler, L. J. Unpublished results.

(21) Davies, P. B.; Russell, D. K. *Chem. Phys. Lett.* **1979**, *67*, 440.

(22) Durig, J. R.; Li, Y.; Shen, S.; Durig, D. T. *J. Mol. Struct.* **1998**, *449*, 131.

(23) Liu, Y.; Butler, L. J. *J. Phys. Chem. A*, to be submitted for publication.